

## **Crystalline–Amorphous Interface Packings for Disks and Spheres**

**Frank H. Stillinger<sup>1</sup> and Boris D. Lubachevsky<sup>1</sup>**

*Received December 14, 1992; final July 16, 1993*

---

We have employed a computer simulation method for uniaxial compression to create random, but spatially inhomogeneous, disk and sphere packings in contact with exposed faces of their own close-packed crystals. The disk calculations involved 7920 movable particles, while the sphere cases utilized over 4000 particles. Rates of compression to the jamming limit were varied over two orders of magnitude, and in three dimensions this produced a clear distinction between the cases of jamming against (001) and (111) faces of the sphere crystal. Specifically, epitaxial order next to the (001) face was markedly enhanced by slowing the compression; for the (111) face the epitaxial order was quite insensitive to the compression rate.

---

**KEY WORDS:** Rigid disks; rigid spheres; amorphous solids; glasses; epitaxial order; crystallization; interfaces.

### **1. INTRODUCTION**

The power of statistical mechanics to describe the behavior of real matter stems in large part from its capacity to exploit simple models. The rigid sphere model (and its two-dimensional rigid disk relative) have certainly been prominent in this regard.<sup>(1–6)</sup> They are sufficiently rich to offer insights into the nature of dense fluids, amorphous solids, and the freezing transition. The present study touches aspects of all of these.

Our prior work has focused on the geometrical properties of random disk and sphere packings,<sup>(7,8)</sup> and has added to a growing literature of such studies.<sup>(9–15)</sup> The principal motivation behind these investigations has been the desire to understand the atomic structure of noncrystalline solids as a form of bulk matter. However, the emphasis in the present paper concerns

---

<sup>1</sup> AT & T Bell Laboratories, Murray Hill, New Jersey 07974, U.S.A.

the interfaces between crystalline and amorphous regions, both of which are geometrically packed (i.e., jammed). We believe the results may have relevance to the kinetics of crystal growth from strongly supercooled liquids and glasses, and to the mechanical strength of "welds" between macroscopic crystalline domains.

The properties of random disk and sphere packings are sensitive to the method used in their formation, in particular, whether sequential addition or full-system compression is selected. This distinction is vital in the present context, since the usual sequential addition method can yield only crystalline packings for some substrate selections, rather than crystalline–amorphous interfaces.

Section 2 presents our computational procedure, involving selection of a fixed substrate array and a dynamical protocol for jamming particles against this array. Section 3 describes results obtained for rigid disks. Sections 4 and 5 report sphere results, respectively, for packing against (001) and (111) substrate crystal faces. The concluding Section 6 interprets our findings in the light of earlier literature on random packings, and in terms of application to real materials phenomena.

## 2. COMPUTATIONAL PROCEDURE

The objective is to produce randomly jammed arrangements of large numbers of disks or spheres in contact with a close-packed crystal surface composed of the same kind of particle. For this purpose we used rectangular (disks) and rectangular-solid (spheres) cells to contain the particles. A single layer of immovable particles stretches across the center of the cell, presenting the desired crystal face to the movable particles above and below. Periodic boundary conditions apply in all directions normal to the cell faces. For a given number of particles the cell is initially chosen to be sufficiently elongated in the direction perpendicular to the fixed crystal surface so as to correspond to a relatively dilute fluid. Figure 1 illustrates this initial geometry. Jamming is produced by shrinking the length of the cell normal to the fixed layer (until the available configuration space undergoes dimensional reduction<sup>(7,8)</sup>).

Our disk calculations have involved 8000 particles, including those forming the fixed crystal layer. This layer consisted of 80 disks. The initial dimensions of the system cell were  $L_x \times L_y \cong 80 \times 400$  in the natural units of particle diameter. The latter dimension can never shrink below  $50 \cdot 3^{1/2}$ , the value it would have if all 8000 particles attained a perfect triangular crystalline array. Such an ideal (but uninteresting!) structure might indeed appear if the rate of compression were very slow (although this is not

inevitable<sup>(8)</sup>). But we have utilized relatively rapid compression to guarantee jamming in a defective structure with a greater final vertical dimension.

Two distinct sphere cases have been examined, corresponding to jamming at distinct crystal faces of the basic face-centered cubic sphere packing. The (001) face comprised  $13^2 = 169$  fixed spheres arranged in contact in a simple square array; the initial cell dimensions were  $13 \times 13 \times 100$  and a total of 4225 particles was involved. The (111) face consists of a close-packed layer of 168 fixed particles (14 rows of 12 spheres); this case utilized a total of 4200 particles with initial cell dimensions  $12 \times 7 \cdot 3^{1/2} \times 100$ .

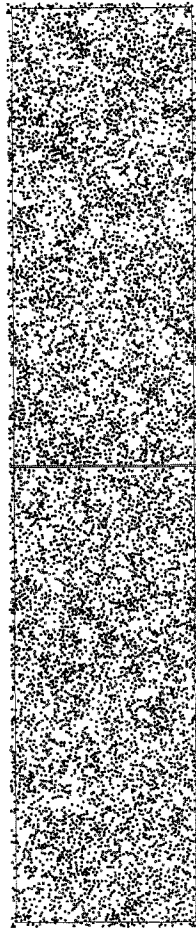


Fig. 1. Initial configuration for production of random disk packing next to a perfect crystal surface. For the case shown the surface consists of 80 disks in contact across the middle of the rectangular cell, and the vertical height is 400 disk diameters.

Preparation of initial conditions employed our procedure for growing a preset number of movable particles<sup>(7,8)</sup> from zero diameter to a small size, relative to jamming, in a fixed orthogonal cell. This cell was then split in the middle, the two halves moved apart, and the fixed layer of particles inserted in the gap.

The subsequent evolution of the system computationally is carried out as a lengthy sequence of "sessions." Each of these follows standard periodic-boundary-condition particle dynamics, encompassing  $5 \times 10^5$  pairwise collisions, except for one fundamental change. This change is produced by the fixed-rate shrinkage of the initially elongated dimension of the system normal to the fixed layer. Consequently, any particle which crosses the top or bottom boundary of the system (and then reappears at bottom or top, respectively, due to periodic boundary conditions) receives a velocity increment equal to twice the boundary velocity. As a result the kinetic energy of the system of movable particles increases during the compression, and would diverge in the jamming limit<sup>(8)</sup> if nothing intervened to prevent it.

On account of this last point, particle velocities are scaled downward at the beginning of each session to keep the kinetic energy bounded. In particular, the mean magnitudes of velocity components normal and tangential to the fixed layer are scaled to be equal and to yield mean value unity for particle speed.

Upon approaching the jamming limit most particles diffuse slowly and collide repeatedly with the same small set of nearest neighbors. This would consume the major portion of the computing activity without leading to any substantial or permanent change in particle arrangement. In a nearly jammed random packing, furthermore, this effect will vary considerably among particles, since some will be tightly confined, while others will reside in looser geometric circumstances. In order to facilitate the computations in their later stages, subsets of particles are identified as those simply executing rapid, small-displacement, collision sequences within a cage formed by a constant set of neighbors; these are temporarily held fixed during the subsequent session while the "looser" particles move. The set of jammed particles held fixed tends to increase from one session to the next; but to avoid total kinetic arrest, all previously fixed particles are freed when four sessions occur in sequence with identically the same set of fixed particles.

Finally, it has been computationally helpful, without significant structural consequences for the final state, to slow the compression rate of the cell in the late stage by a factor of  $10^2$ . This and the preceding tactics provide an effective way to approach the strict jamming limit to high numerical precision.

### 3. RIGID DISKS

The 8000-disk system depicted in Fig. 1 was subjected to vertical compression at a rate very large compared to the initial mean particle speed, namely

$$dL_y/dt = -1000 \quad (3.1)$$

Figure 2 shows the system at an intermediate stage, with the disks in a dense but not yet jammed state. Those disks in the immediate vicinity of the fixed line of 80 exhibit a substantial degree of epitaxial order. But at the same time the beginnings of polycrystalline order have begun to emerge in regions somewhat farther from the fixed line, with orientations in conflict with an epitaxial array.

Figure 3 presents the final jammed state. The fraction of the entire system area covered by the 8000 disks in this state (the "packing fraction") is

$$\xi = 0.865513475 \quad (3.2)$$

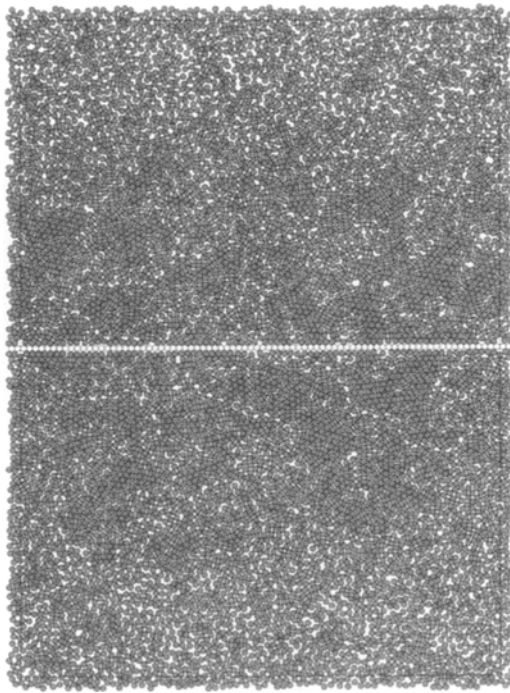


Fig. 2. Intermediate stage in rapid compression of the 8000-disk system. The packing fraction is 0.72646489 [maximum value, for the triangular crystal, is  $\pi/(2 \cdot 3^{1/2}) = 0.906899682$ ].

This may be compared with the maximum value of  $\xi$ , attained with a perfect triangular lattice:

$$\xi_{\max} = \pi/(2 \cdot 3^{1/2}) = 0.906899682\dots \quad (3.3)$$

The disk pattern in Fig. 3 away from the fixed line is qualitatively similar to those that have been generated previously under rapid jamming conditions.<sup>(7,8)</sup> It can be described as polycrystalline, with individual grains often traversed by shear-generated linear faults, and occasionally containing vacancies. The conflicting growth directions of the epitaxial layers above and below the fixed line, and of the neighboring misoriented grains, has now become visually very obvious. The vertical range of epitaxial order appears to be less than the mean grain diameter in the regions away from the "crystal surface."

Careful examination of the configuration depicted in Fig. 3 reveals that not all disks in contact with the fixed row of 80 reside precisely in "pockets" of that row (i.e., in simultaneous contact with two of its disks). Instead there can exist a small lateral displacement, with corresponding

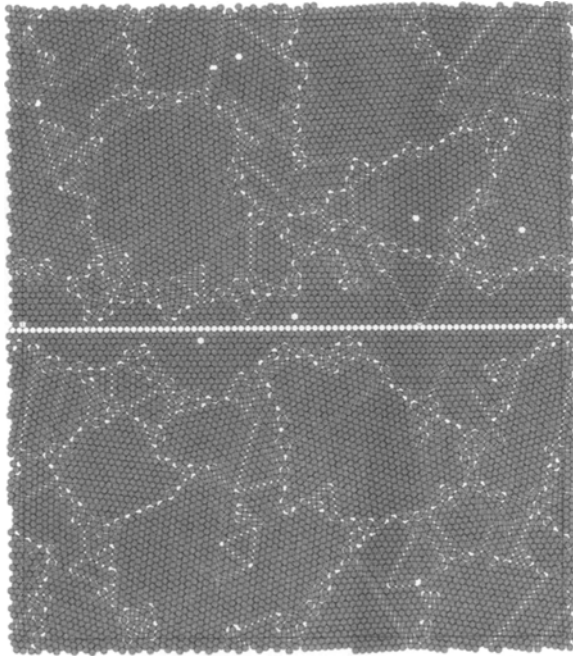


Fig. 3. Jammed state produced by completed compression of the configuration shown in Fig. 2. The packing fraction is 0.865513475.

uplift. A clear indication of this feature is the V-shaped intrusion just above the fixed row, one-quarter its length from the right end in Fig. 3. In order for this to be jammed in place, the epitaxial material to its left and right must be slightly displaced inward toward the center line of the intrusion.

The packing fraction shown in Eq. (3.2) falls in the range for rapidly jammed bulk disk packings.<sup>(7,8)</sup> It is also useful to record the slightly modified packing fraction that emerges from application of the Gibbs dividing surface concept.<sup>(16)</sup> In the present circumstance this requires surrounding the fixed row symmetrically with a strip whose area  $A_s$  is equal to that attributable to 80 disks embedded within a perfect close-packed crystal:

$$A_s = 80(3^{1/2}/2) = 40 \cdot 3^{1/2} \quad (3.4)$$

Then the total system area  $A$  minus  $A_s$  is the appropriate area "belonging" to the 7920 initially movable disks that actually form the amorphous phase, and their corresponding packing fraction is

$$\xi' = 0.865114694 \quad (3.5)$$

The disk packing displayed in Fig. 3 is but one of several that have been produced by the method described above. Although details differ slightly from case to case, the qualitative features mentioned for Fig. 3 appear to be generally applicable.

Finally, it is worth stressing that a conventional sequential process for adding disks atop a fixed crystal surface would produce results quite different from those just discussed. In particular, one popular method brings particles one at a time to the growing aggregate in a direction normal to the surface, and after contact, sliding the particle downward into a pocket.<sup>(17)</sup> For the case of disks growing on the type of fixed row used here, the result invariably would be a perfect close-packed crystal, devoid even of isolated vacancies.

#### 4. SPHERES ON A (001) FACE

As explained in Section 2, this three-dimensional case involves 169 fixed spheres forming the exposed crystal face, and 4056 movable spheres of the same unit-diameter size. Two examples will be discussed, differing in the rate at which the initially elongated cell was shortened:

$$\begin{aligned} dL_z/dt &= -1.00 && \text{(rapid jamming)} \\ &= -0.01 && \text{(slow jamming)} \end{aligned} \quad (4.1)$$

The respective final states possessed the following packing fractions:

$$\begin{aligned}\xi &= 0.663743666 && \text{(rapid jamming)} \\ &= 0.703345180 && \text{(slow jamming)}\end{aligned}\quad (4.2)$$

which can be compared with the close-packed value:

$$\xi_{\max} = \pi/(3 \cdot 2^{1/2}) = 0.7404804897\dots \quad (4.3)$$

If we adapt the Gibbs dividing surface concept,<sup>(16)</sup> invoked previously for disks, to excise the volume attributable to the ordered surface particles, we find in place of Eq. (4.2) the slightly reduced values

$$\begin{aligned}\xi' &= 0.660889967 && \text{(rapid jamming)} \\ &= 0.701878538 && \text{(slow jamming)}\end{aligned}\quad (4.4)$$

In a manner analogous to that found for disks in two dimensions, the sphere packings experience epitaxial ordering near to the fixed surface, but show disorder further away. One convenient way to visualize this phenomenon is illustrated by Fig. 4. It shows, for the rapidly compressed

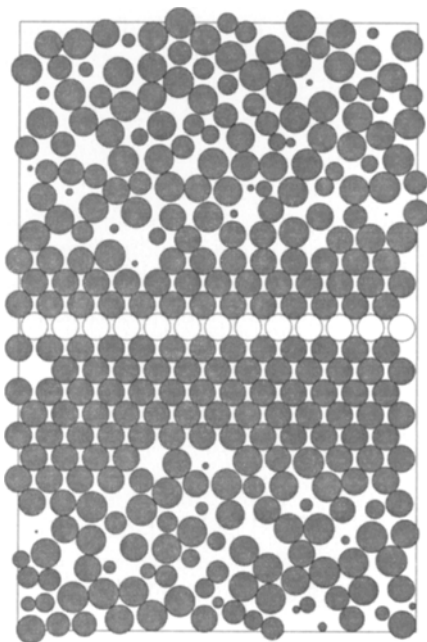


Fig. 4. Planar section through the rapidly compressed sphere packing, in contact with a fixed (001) sphere array (open circles).

case, a planar section through the jammed packing that is normal to the surface. Circular slices through the initially mobile spheres are shaded, those through the surface particles are unshaded. Decay of positional order away from the surface is obvious.

Near the left-hand margin in Fig. 4, in the second ordered layer below the fixed surface, one encounters a monovacancy (missing sphere). These point defects seem to occur rather frequently in epitaxially ordered regions when rapid compression has been employed to jam up the collection of spheres. Figure 5 provides another monovacancy example from the same jammed packing, this time in the layer immediately above the fixed surface. The sectioning plane used is parallel to that of Fig. 4, but displaced from it by one sphere diameter.

By contrast to the vivid domain texture of the disk packing away from its fixed surface (Fig. 3), various views of the sphere packing, such as provided by Figs. 4 and 5, reveal no tendency toward formation of crystalline domains outside of the epitaxially ordered region in the immediate vicinity of the fixed surface. This is consistent with our prior observations

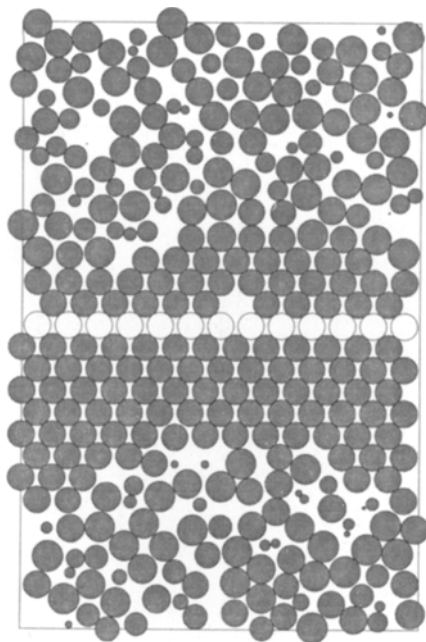


Fig. 5. Another planar section through the rapidly compressed packing at a fixed (001) sphere array. This section is parallel to that of Fig. 4, but displaced by 1 unit (sphere diameter).

on sphere packings created in the absence of fixed surface arrays.<sup>(8)</sup> As a consequence, we do not expect, and have been unable to identify, discrete cavities in the amorphous regions of the high-compression-rate packing that by their size could legitimately be termed “vacancies.”

Another way to view heterogeneous sphere packings of the kind under consideration focuses on the variation of density with respect to position. Figure 6 exhibits, in histogram form, the density of sphere centers as it varies with normal distance from the fixed square array of 169 spheres. Once again this refers to the packing produced by rapid compression. The peak at the origin comprises the fixed layer, and it is surrounded on either side (as expected) by several peaks of nearly equivalent magnitude. This is followed by a rapid decay into an essentially flat distribution within the amorphous packing regions.

The bins utilized for Fig. 6 have widths equal to one-eighth the layer spacing in the (001) direction for a perfect close-packed (face-centered cubic) crystal. If indeed such a crystal were present, the distribution would have consisted only of isolated peaks, all equal in height to that at the origin. The failure of close-in peaks of Fig. 6 to attain the height of the one at the origin stems in part from the presence of vacancies, as already mentioned. But it is also due to the displacement of a few particles out of the crystal positions into neighboring bins. Note that these displacements are almost always in the direction *away* from the fixed surface. This asymmetry represents a three-dimensional analog for the “uplift” phenomenon discussed earlier for disks in two dimensions.

Figures 7 and 8 are the analogs of the prior Figs. 4 and 5, but now for the more slowly compressed packing in contact with the fixed (001)

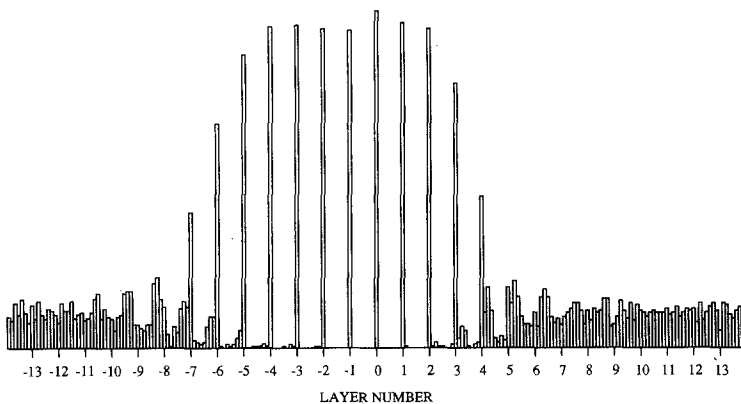


Fig. 6. Density distribution of sphere centers normal to the fixed (001) array (located at the origin). This result refers to the rapidly compressed packing.

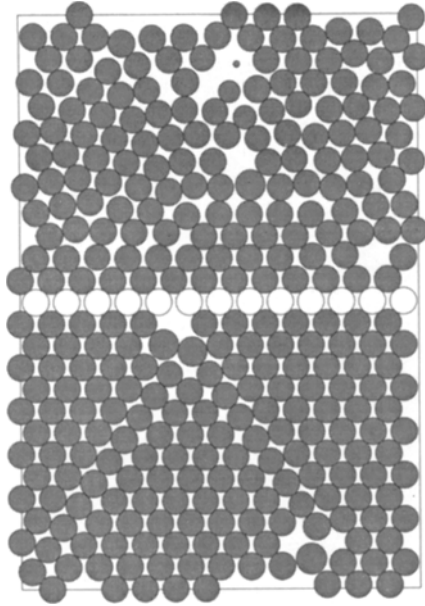


Fig. 7. Planar section through the slowly compressed packing at a fixed (001) sphere array, oriented normal to that array (open circles).

array. These planar sections, again normal to the fixed array, illustrate the reason why the final jamming density has increased [Eqs. (4.2) and (4.4)]. It is clear, particularly by viewing the bottom half of Figs. 7 and 8, that a greater extent of epitaxial order has appeared. Evidently the longer time available to the movable spheres before they become substantially locked in place has permitted them to anneal out some of the stacking disorder.

The density distribution normal to the fixed array for this slow-compression case appears in Fig. 9. It stands in strong contrast to the rapid-compression version in Fig. 6. No region now appears in which the sphere density is substantially constant; strong oscillations appear all the way across the periodic boundary from the fixed array to its image. Indeed this stratification is so well developed that empty histogram bins exist between each pair of layer peaks. Even though the ordering is imperfect, it appears that this slow-jamming regime encourages orientational ordering of at-least-partially-crystalline domains that are translationally a bit out of register with the perfect epitaxial material.

Both density distributions, Figs. 6 and 9, display asymmetry about the fixed layer at the origin. This is particularly obvious in the latter case. It is a characteristic arising from the modest system sizes to which we are confined by the practical limitations of computing resources. The coherence

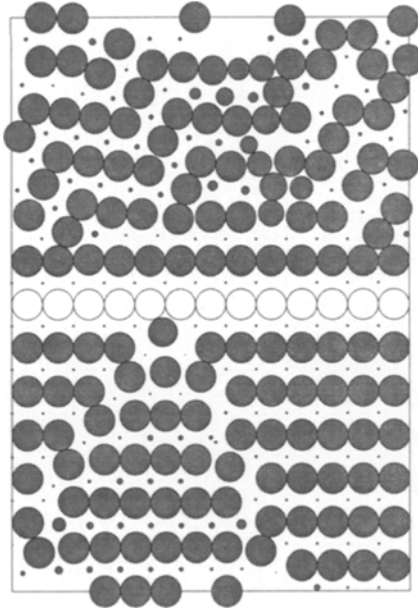


Fig. 8. Another planar section through the slowly compressed packing at a fixed (001) sphere array. This section is parallel to that of Fig. 7, but displaced by 3.75 units (sphere diameters).

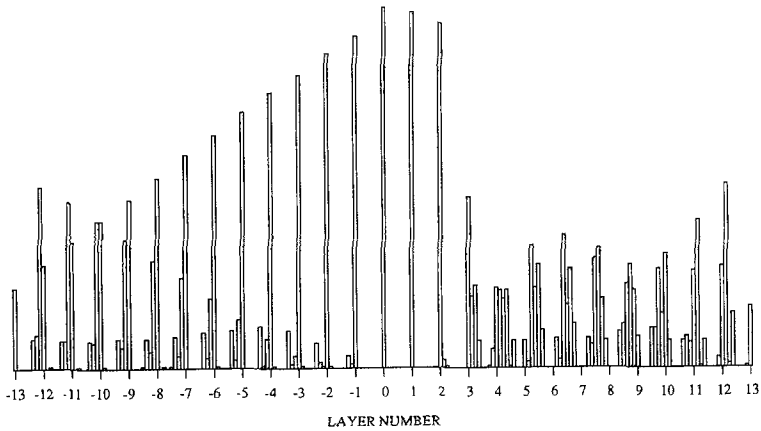


Fig. 9. Density distribution of sphere centers, normal to the fixed (001) array, for the slowly compressed packing.

lengths of ordered regions are comparable to lateral dimensions of the box size used. If it were possible to increase system size without limit, symmetry should be restored with unit probability.

## 5. SPHERES ON A (111) FACE

Now we consider sphere packing against a close-packed layer of 168 fixed spheres. The movable spheres number 4032, and once again have the same unit diameter as those that are fixed. As was the case in Section 4 for the (001) crystal face, both rapid and slow compressions have been examined. The respective compression rates are the same as those shown earlier in Eq. (4.1).

The final jammed states were found to possess the following overall packing fractions:

$$\begin{aligned} \xi &= 0.640745982 && \text{(rapid jamming)} \\ &= 0.638844252 && \text{(slow jamming)} \end{aligned} \quad (5.1)$$

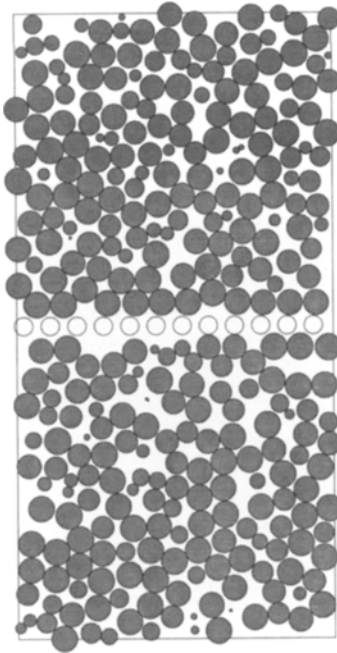


Fig. 10. Planar section, normal to a fixed (111) surface, through a rapidly compressed sphere packing.

By invoking once again the Gibbs dividing surface strategy to remove the effect of the ordered fixed layer, these packing fractions are replaced with the smaller values

$$\begin{aligned}\xi' &= 0.637170159 && \text{(rapid jamming)} \\ &= 0.635211447 && \text{(slow jamming)}\end{aligned}\tag{5.2}$$

Notice that this set of packing fractions is uniformly smaller than those presented in Section 4, Eqs. (4.2) and (4.4), and within expected statistical dispersion essentially independent of compression rate.

Figures 10 and 11 begin to reveal the reason for the last observation. They provide a pair of parallel planar sections through the rapidly compressed packing, normal to the fixed (111) array of spheres, and separated by 1.5 units, approximately. In distinct contrast to Figs. 4, 5, 7, and 8, very little epitaxial ordering appears. The reason evidently stems from a basic distinction between the crystal growth processes at (001) and (111) surfaces. In the former case every pocket formed by a square of spheres in the

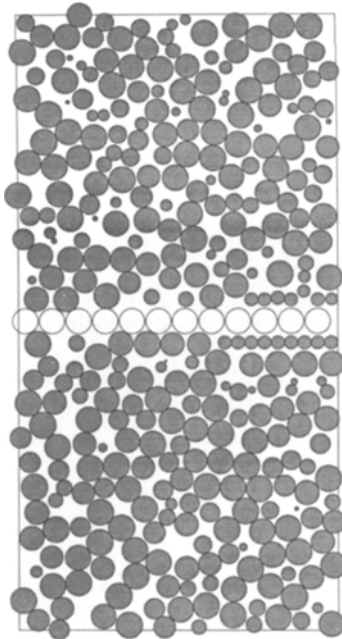


Fig. 11. Another planar section through the rapidly compressed sphere packing at a fixed (111) surface. This is parallel to that of Fig. 10, but displaced by approximately 1.5 sphere diameters.

underlying layer can and must be occupied by a sphere in formation of a next crystal layer. But in the latter case the pockets are triangular, and only every second one will be filled by the completed next layer. This degeneracy leads to stacking faults (ref. 18, p. 637) and dislocations (ref. 18, p. 628) that disrupt orderly propagation of the crystal structure, and almost immediately lead to amorphous sphere arrangement as distance increases from the fixed (111) triangular array.

The stacking ambiguity next to the fixed layer is confirmed by examining sections parallel to that layer. Figure 12 presents a good example, also from the rapidly jammed case. The section shown is located below the fixed array at the position of the centers of a perfect epitaxial layer resting just underneath that fixed array [downward displacement  $-(2/3)^{1/2}$ ]. Although the sphere positions indicated show some disorder, they also include close-packed triangular patches. However, these patches are out of registry with one another because their spheres have settled into distinct pocket subsets. This is seen most clearly near the figure's right edge. The "channels" between neighboring patches are dislocation cores into which subsequent layers of spheres can deeply penetrate.

Figure 13 presents the density variation in this rapidly jammed packing as a function of distance from the fixed (111) array. While some epitaxial stratification appears, it extends substantially less far than for the (001) cases discussed in Section 4.

In contrast to the (001)-surface cases, slowing the jamming rate has relatively little structural influence in the present case of the fixed (111)

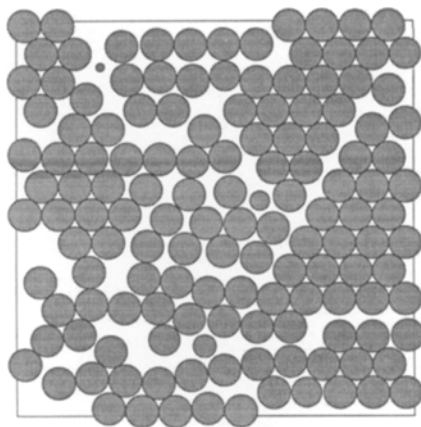


Fig. 12. Planar section, parallel to the fixed (111) surface, through the rapidly compressed sphere packing. The position coincides with that of sphere centers in a structurally perfect layer just below the fixed sphere array.

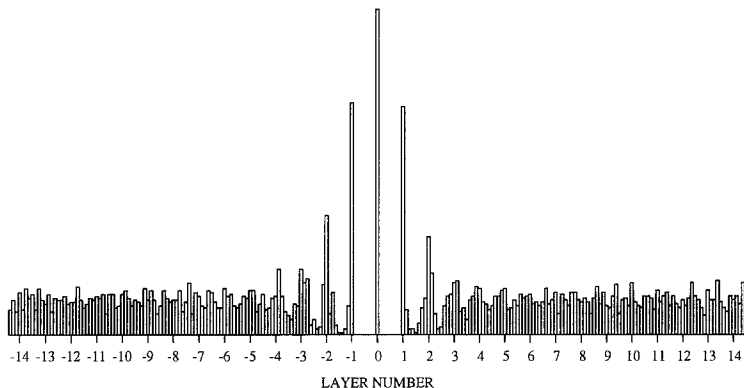


Fig. 13. Density variation normal to the fixed (111) array for the rapidly compressed sphere packing.

surface. Figure 14 shows the resulting normal-direction density variation. While small details distinguish the histograms in Figs. 13 and 14, the overall patterns are nearly the same. This is consistent with the near equality of packing fractions for rapid and for slow compression with this surface. Although not shown here, examination of normal and parallel direction sections for the slow-compression case are qualitatively very similar to those of the rapid-compression case. If indeed it is possible to eliminate stacking fault disorder at the (111) surface by annealing, it apparently can only occur with much slower compression rates than we have considered thus far.

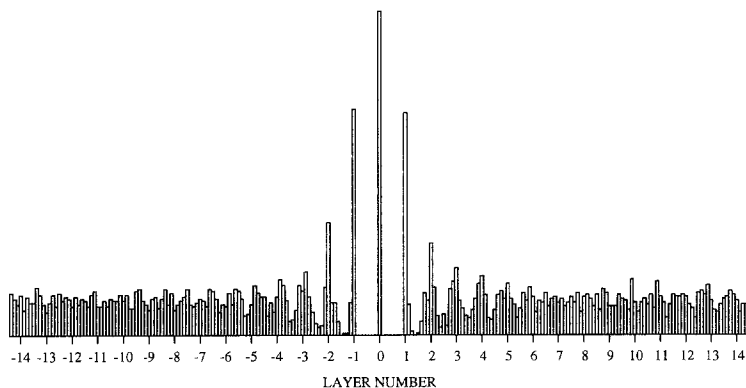


Fig. 14. Density variation normal to the fixed (111) array for the slowly compressed sphere packing.

## 6. DISCUSSION

One of the achievements of the present project is simply the demonstration that disk and sphere packings exist with an interface between ordered crystalline and disordered amorphous regions. This is no surprise for spheres pressed against a (111) face of the close-packed sphere crystal; as discussed in Section 5, stacking faults and associated dislocations disrupt orderly extension of the periodic crystal structure into the region of added spheres. However, the existence of inhomogeneous (crystal–amorphous) packings for disks in two dimensions and for spheres jammed against a (001) crystal face in three dimensions is not *a priori* obvious. Packings produced by conventional sequential addition procedures in these latter two cases invariably extend the underlying crystalline layering into the growing region without limit, and produce perfect stratification. The compressive jamming procedure used in the present study shows that this kind of outcome is not inevitable.

The published literature concerning disk and sphere packings often presents the concept of densest “random close packing,” with the suggestion that unique densities can be identified for these in two and three dimensions.<sup>(11,14,19–21)</sup> The results reported in this and our previous<sup>(7,8)</sup> papers suggest the contrary. Random disk packings have a distinctly polycrystalline texture, and the mode of formation can be used to control the mean linear grain size to lie anywhere between a few disk diameters to arbitrarily large size. As a result the packing density can be varied continuously (in the large-system limit) over at least the range<sup>(8)</sup>

$$0.852 < \xi \leq \pi/(2 \cdot 3^{1/2}) \quad (6.1)$$

where the upper limit corresponds to the perfect triangular crystal. Indeed the lower limit in Eq. (6.1) probably can be reduced substantially by incorporating high concentrations of monovacancies in the crystalline grains.

Surely an analogous situation obtains for the packing of spheres in three dimensions. We have established in the present work (successfully placing amorphous packings next to a crystal face) that crystalline domains, apparently of arbitrary size, can coexist stably with disordered regions. In the large-system limit it should be possible to vary the proportion of these two types of regions continuously. As a consequence, the packing density likewise will vary continuously up to the maximum attainable, corresponding to the perfect cubic close-packed crystal. The “unique” random close-packed densities that seem to emerge from various prior studies are simply characteristics of the specific preparation method employed.

A possibly significant extension of the work reported here would involve incorporation of a small fraction of "impurity" spheres differing in size from the majority. Particularly in the case of jamming at the (001) crystal face where substantial epitaxial ordering of the uniform-size sphere system was observed (Section 4), the results in the extension should depend sensitively on whether the impurity spheres were smaller or larger than the rest. In the small-impurity case, simple substitution of a few spheres should occur, creating "impurity rattlers," but not otherwise disturbing the epitaxial stratification. But larger impurities would not fit without disrupting the epitaxial order. If the rate of compression to the jamming limit is rapid, the larger impurities would tend to be trapped in the interfacial zone and would inhibit outward growth of the crystalline order. Slow compression, on the other hand, might permit diffusive expulsion of impurities from the interfacial zone as in zone refining,<sup>(22)</sup> thus restoring the possibility of substantial crystalline ordering.

## REFERENCES

1. S. Chapman and T. G. Cowling, *The Mathematical Theory of Non-Uniform Gases* (Cambridge University Press, Cambridge, 1953), Chapters 5 and 6.
2. H. L. Frisch, *Adv. Chem. Phys.* **6**:229 (1964).
3. K. Huang and C. N. Yang, *Phys. Rev.* **105**:767 (1957).
4. T. D. Lee, K. Huang, and C. N. Yang, *Phys. Rev.* **106**:1135 (1957).
5. B. J. Alder and T. E. Wainwright, *J. Chem. Phys.* **31**:459 (1959).
6. L. V. Woodcock, *Ann. N.Y. Acad. Sci.* **371**:274 (1981).
7. B. D. Lubachevsky and F. H. Stillinger, *J. Stat. Phys.* **60**:561 (1990).
8. B. D. Lubachevsky, F. H. Stillinger, and E. N. Pinson, *J. Stat. Phys.* **64**:501 (1991).
9. P. H. Gaskell, in *Glassy Metals*, H. Beck and H.-J. Güntherodt, eds. (Springer, Berlin, 1983), Vol. II, pp. 5–49.
10. C. H. Bennett, *J. Appl. Phys.* **43**:2727 (1972).
11. J. L. Finney, *Nature* **266**:309 (1977).
12. D. J. Adams and A. J. Matheson, *J. Chem. Phys.* **56**:1989 (1972).
13. F. Delyon and Y. E. Lévy, *J. Phys. A* **23**:4471 (1990).
14. E. L. Hinrichsen, J. Feder, and T. Jossang, *Phys. Rev. A* **41**:4199 (1990).
15. A. Pavlovitch, R. Jullien, and P. Meakin, *Physica A* **176**:206 (1991).
16. J. S. Rowlinson and B. Widom, *Molecular Theory of Capillarity* (Clarendon Press, Oxford, 1982), p. 31.
17. W. M. Visscher and M. Bolsterli, *Nature* **239**:504 (1972).
18. N. W. Ashcroft and N. D. Mermin, *Solid State Physics* (Saunders, Philadelphia, 1976).
19. J. G. Berryman, *Phys. Rev. A* **27**:1053 (1983).
20. J. Tobochnik and P. M. Chapin, *J. Chem. Phys.* **88**:5824 (1988).
21. J. Nezbeda and W. R. Smith, *Mol. Phys.* **75**:789 (1992).
22. W. G. Pfann, *Zone Melting* (Wiley, New York, 1958).